



Title	Laser Rapid Solidification Microstructure in Single Crystals of Al and Al-2% Cu Alloys(Materials, Metallurgy & Weldability)
Author(s)	Matsunawa, Akira; Katayama, Seiji; Simidzu, Hiroyuki
Citation	Transactions of JWRI. 1990, 19(1), p. 67-77
Version Type	VoR
URL	https://doi.org/10.18910/12630
rights	
Note	

The University of Osaka Institutional Knowledge Archive : OUKA

<https://ir.library.osaka-u.ac.jp/>

The University of Osaka

Laser Rapid Solidification Microstructure in Single Crystals of Al and Al-2%Cu Alloys[†]

Akira MATSUNAWA^{*}, Seiji KATAYAMA^{**} and Hiroyuki SIMIDZU^{***}

Abstract

Characteristics of rapid solidification were investigated in detail in terms of microstructure, solidification modes, growth crystallography and microsegregation by irradiating a pulsed Nd: YAG laser on the specific surfaces (001) (011) and (111) of single crystals of pure Al and Al-2%Cu alloys. In laser spot weld fusion zones of both alloys, epitaxial growth occurred as planar interface and then cellular or cellular dendritic interface from the unmelted semi-spherical base metal inwards. Also a number of grains were formed as "stray" crystals in the upper part of shallow fusion zones and in central part of deep fusion zones in Al-2%Cu alloy. In pure Al, cells had the same crystallographic orientation as the base metal. However, in Al-2%Cu, the crystallographic orientations of cells were several degrees different from those of the base metal. The growth direction of cell trunks in pure Al was gradually shifted from the $\langle 100 \rangle$ direction toward the directions of heat and liquid flow. In Al-2%Cu, on the other hand, dendritic cell trunks grew straight, which were deviated up to 15° at the maximum from the $\langle 100 \rangle$ to heat flux flow direction immediately after the growth initiation. Moreover, net-like (weave) microstructure of cellular dendrites was observed in boundary zones where cells of different $\langle 100 \rangle$ growth directions impinged. Cu element was likely to segregate at grain and cellular dendritic boundaries, resulting in the formation of Cu-enriched intermetallic phase. It was also confirmed that cracks took place at grain boundaries but not at cellular dendritic boundaries.

KEY WORDS : (Laser) (Rapid Solidification) (Single Crystal) (Aluminum Alloys) (Microstructure) (Microsegregation) (Crystallography) (Growth Direction) (Cracking)

1. Introduction

The laser is a heat source which can produce extremely high power/energy density. Such focused laser beams have been utilized in various materials processing techniques such as transformation hardening, welding, cladding, surface alloying, glazing (rapid solidification surface modification), drilling, etc. Thus a wide variety of microstructures can be formed in such laser techniques¹⁾. Recently, laser rapid solidification (glazing) is receiving considerable attention because rapid solidification (rapid quenching from the molten state) is a means to generate novel microstructures, including very fine microstructures (with small cells or fine eutectic structures), microstructures related to reduced microsegregation, extended solid solutions, metastable crystalline phases, amorphous metallic phases, etc., which frequently possess beneficial properties¹⁻¹⁴⁾. Also, rapid solidification theories have been developed in order to understand a variety of microstructures and microsegregation¹⁵⁻¹⁸⁾. The theories permit predicting the representation of calculated dendrite tip radius and calculated dendrite tip temperature as a function of dendrite growth velocity, the velocities for the

stability limit of the planar front and the absolute stability limit, etc. for some alloys. However, the theories require further experimental investigation and verification of rapid solidification.

On the other hand, in the case of normal solidification, especially in conventional castings, the solidification morphologies such as planar, cellular, cellular dendritic and columnar dendritic interface solidification and equiaxed solidification are interpreted by considering the dependence on alloy composition, and temperature gradient and solidification rate (velocity)¹⁹⁾. Also, in the face-centered and body-centered cubic metals and alloys, the preferred growth directions of dendrites are $\langle 100 \rangle$. Dendrites will grow in that preferred crystallographic direction which is closest to the heat flow direction, while cells grow with their axes parallel to the heat flux direction without regard to the crystal orientation¹⁸⁾. The growth direction of a dendritic cell is approaching to this easy growth direction as the growth rate increases and as the amount of solute atoms becomes larger²⁰⁻²²⁾.

Furthermore, in conventional arc and resistance welding, it has been well known that the solidification microstructure and microsegregation in a weld exert a

[†] Received on May 8, 1990

^{*} Professor

^{**} Instructor

^{***} Kobe Steel Corporation, Ltd.

Transactions of JWRI is published by Welding Research Institute of Osaka University, Ibaraki, Osaka 567, Japan

great influence upon the hot cracking sensitivity and mechanical properties of the weld metal. Thus the solidification structures and solidification mechanisms of the weld metal were investigated by Matsuda, et al²³⁻²⁶, Savage, et al²⁷⁻²⁹, and others^{30,31}. It is well understood that initial solidification within the weld fusion zone occurs epitaxially as a planar interface solidification from the partially melted grains along the fusion boundary, leading to the variation to cellular and/or cellular dendritic interface solidification with a decrease in temperature gradient and an increase in growth rate inward the fusion zone.

In recent years, a few experiments and theoretical investigation have been conducted on the formation mechanism of solidification structure in single crystal alloys subjected to relatively rapid solidification by laser or electron beam welding. Narasimhan, et al³² investigated the microstructure of weld fusion zones in laser-melted single crystal of Ni base superalloy Udimet 700, and reported the characteristics of the solidification structure in the zones. Rappaz, et al³³ performed electron beam welding on the single crystal alloy of Fe-15Ni-15Cr (Ni: $k_0 = 0.9$), and indicated that the measured radius of the dendrite coincided with the theoretical value obtained by the KGT model¹⁶. However, further information and data of microsegregation are needed. Few reports have yet been made on microstructural characteristics, the mechanism of rapid solidification and the behavior of microsegregation in single crystals of a pulsed laser spot weld, although rapid solidification and easier theoretical analysis in a weld fusion zone may be expected.

Therefore, in this study, in order to obtain a basic

knowledge of the mechanisms of rapid solidification and microsegregation, the characteristics of the rapid solidification microstructure and the relationship between rapid solidification behavior and growth crystallography were investigated by irradiating pulsed Nd: YAG laser beam on the surfaces with particular orientations of single crystal pure Al and Al-2%Cu alloy. The reasons for the selection of pure Al and Al-Cu system are as follows: (1) Phase diagram is well established, as shown in Fig. 1. (2) Microsegregation is likely to occur due to small distribution coefficient ($k_0 = 0.15$), and consequently hot cracking may take place. (3) Cu is very important as precipitation hardenable element in Al alloys. (4) Single crystal can be prepared easily.

2. Materials Used and Experimental Procedures

The materials used are pure Al and Al-Cu alloy. The chemical compositions of the alloys are shown as ① and ③ in Table 1. This Al-2%Cu alloy (about 1 kg) was produced by melting the mixture of pure Al ① and Al-50%Cu ② alloys in the graphite crucible in Ar atmosphere using high frequency induction furnace.

Crystal grains of pure Al and Al-Cu alloy were grown to be approximately 15 mm by using strain annealing technique. The orientation of the grains were determined by Laue back reflection X-ray technique (35 kV, 12 mA, 50 min). These large grains were cut into 3 mm thick single crystal specimens having the surfaces of (001), (011) and (111) crystallographic planes by abrasive slurry wire saw. Specimen surfaces were polished with #400 emery paper, acid-cleaned, and cleansed with acetone prior to laser irradiation. Experimental procedure of laser irradiation is schematically shown in Fig. 2. Each specimen was exposed to a pulsed Nd: YAG laser in Ar atmosphere to produce a considerably rapidly solidified spot weld. The laser used was Miyachi Laser System Laser with the

Table 1 Chemical compositions of pure Al and Al-Cu alloy used

		Compositions (wt%)			
		Al	Cu	Fe	Si
①	Pure Al	99.992	0.001	0.004	0.003
②	Al-Cu (Mother Metal)	50.970	48.957	0.073	—
③	Al-2%Cu (①+②)	Bal.	2.12	0.007	0.002

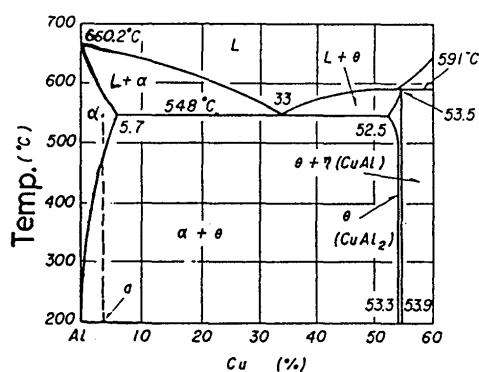


Fig. 1 Phase diagram of Al-Cu System.

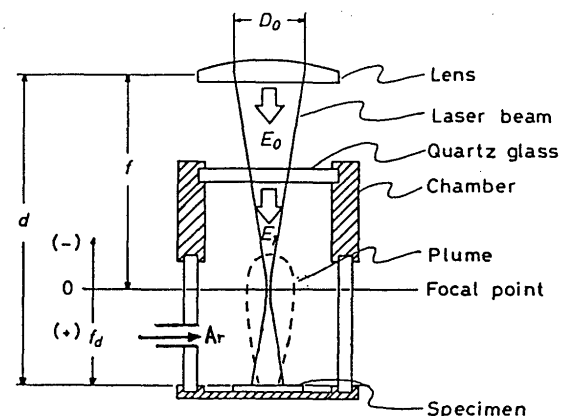


Fig. 2 Experimental configuration for pulsed Nd: YAG laser spot welding of single crystal specimens.

maximum output power of 200 W, the maximum pulse energy of 80 J/P and pulse widths of 0.1 to 10 ms. The conditions of laser irradiation were: a pulse energy, $E_1 = 75$ J/P; a pulse width, $\tau_p = 8$ ms; defocused distance, $f_d = +5$ & $+3$ mm (the focal length of lens, $f = 50$ mm).

Figure 3 shows pulsed laser output characteristics.

Laser spot welds were analyzed by Laue back-reflection X-ray technique again, and the surfaces and special cross sections were observed by optical microscope and scanning electron microscope (SEM) with EDX after etching in Keller's reagent.

3. Experimental Results and Discussion

3.1 Microstructure of heat conduction type penetration welds

Figure 4 shows the surface appearance of the weld fusion zone (a) irradiated by laser beam onto the surface of the plane (011) of Al-2%Cu specimen at the defocused

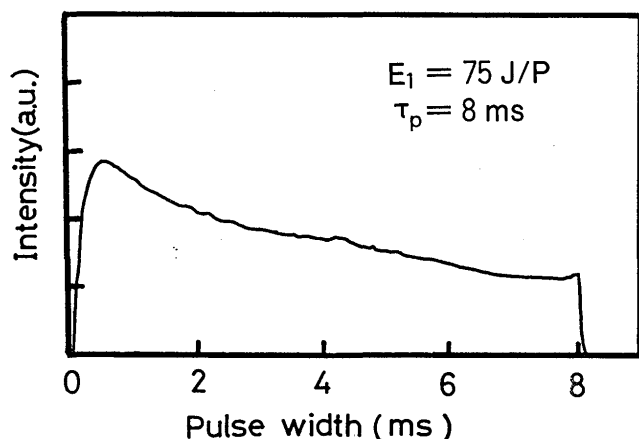


Fig. 3 Output characteristic of pulsed Nd: YAG laser ($E_1 = 75$ J/P, $\tau_p = 8$ ms).

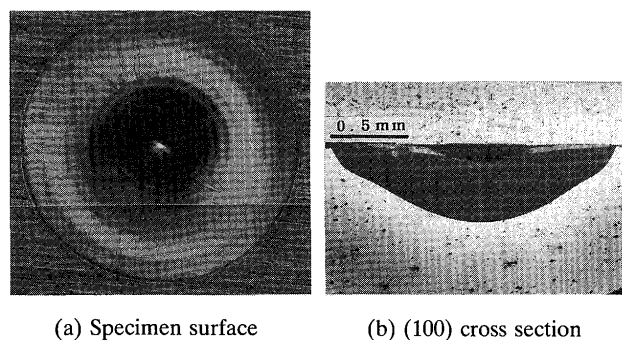


Fig. 4 (011) surface specimen of Al-2%Cu alloy irradiated by pulsed Nd: YAG laser under conditions of $E_1 = 75$ J/P and $f_d = +5$ mm.

distance, $f_d = +5$ mm, and the weld cross section (b) across the center of the fusion zone cut parallel to the plane (100) of the base metal. Figures 5 (a) and (b) show the results of pure Al specimen under the same conditions. In both alloys, shallow penetration of a spot weld (of about 0.5 mm depth and 0.1 mm concavity) was obtained. In Al-2%Cu, new grains of different optical reflection were observed just like "stray crystals" in the upper central part of the fusion zone, whereas in pure Al, an array of needles inward the fusion center and deeply etched zone (presumably due to strong convection or molten flow) were seen on the surface and cross section.

Figures 6 (a) and (b) show the Laue back reflection patterns obtained before and after laser irradiation onto the surface of (011) plane of Al-2%Cu specimen. Figure 6 (c) exhibit the pattern from the specimen of laser weld fusion zone where the upper surface part of stray crystals was removed about 0.1 mm. Also, Figure 7 shows the Laue back reflection patterns from the surface of pure Al specimen before and after laser irradiation.

Before laser irradiation, two $\langle 100 \rangle$ upward and downward directions are on the specimen surface, and the other two $\langle 100 \rangle$ directions are 45° upward with respect to the specimen surface (as referred to Fig. 8). After laser irradiation, for Al-2%Cu, Debye-ring is observed although it disappears for the polished surface, as shown in Figs. 6 (b) and (c), whilst the spots are seen for pure Al. These results confirm that the weld fusion zone in Al-2%Cu is polycrystalline near the surface. This suggests that a number of grains radiating in all directions near the surface of the Al-2%Cu fusion zone are formed as "stray crystals" having no consistency with the crystallographic orientation of the substrate. On the other hand, for the specimen of polished surface, as shown in Fig. 6 (c), weak reflection spots were observed from $\{024\}$ and $\{133\}$ planes only, and spots from other planes were invisible in background. This indicates that the dendritic growth (solidification) direction is slightly different from the preferred growth direction $\langle 100 \rangle$. The spreading angles of

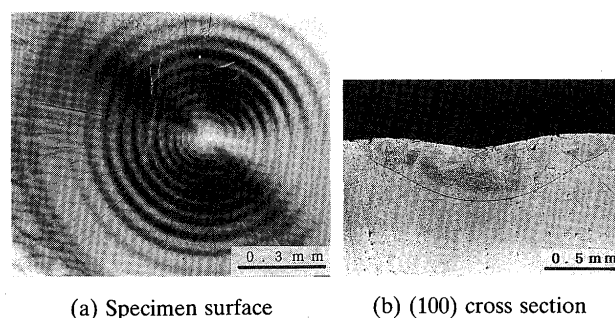


Fig. 5 (011) surface specimen of pure Al alloy irradiated by pulsed Nd: YAG laser ($f_d = +5$ mm, $E_1 = 75$ J/P).

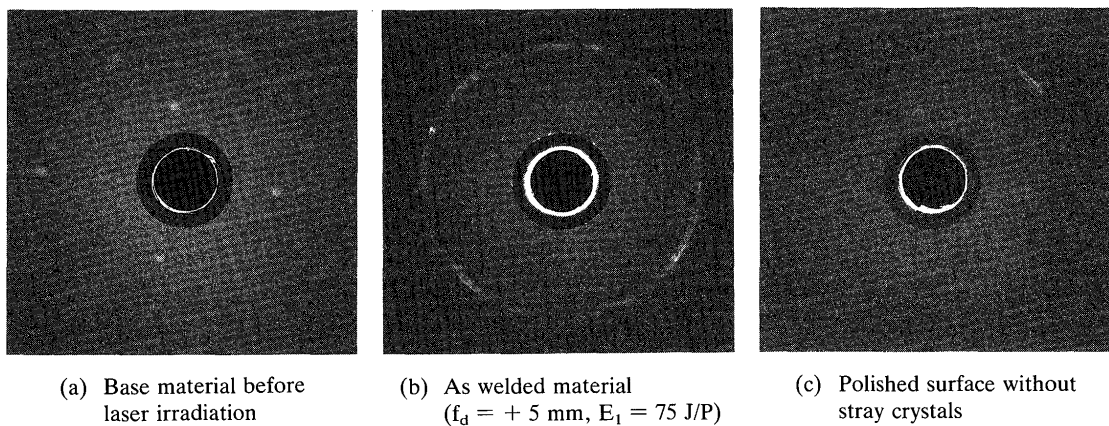
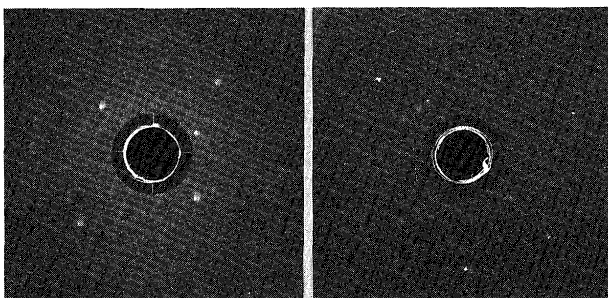


Fig. 6 Laue patterns from Al-2%Cu (011) specimen.

these spots to $\langle 100 \rangle$ direction are about ± 3 degrees. This is new finding and different from the results of Laue patterns obtained from a conventional arc weld²⁶⁾ reporting that the weld metal will solidify as a single crystal having the same crystallographic orientation as the substrate.

Subsequently, solidification microstructure of the laser



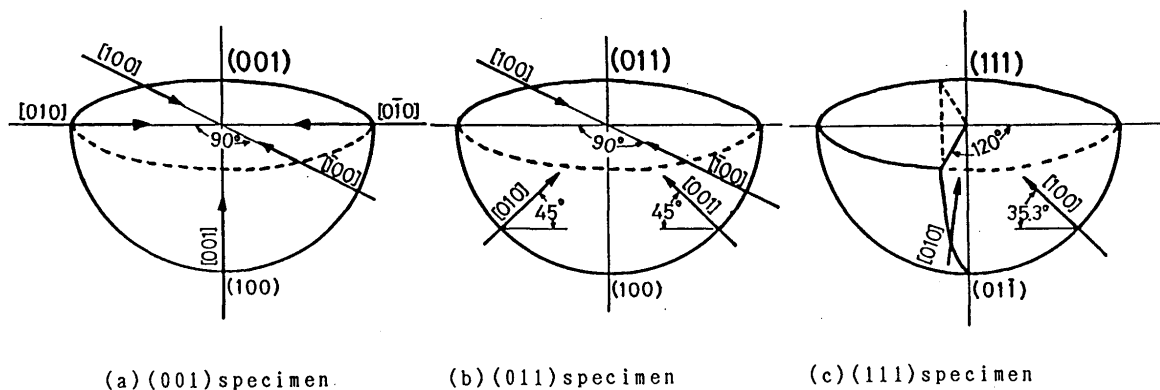
(a) Base material before laser irradiation (b) As-welded material ($f_d = + 5$ mm, $E_1 = 75$ J/P)

Fig. 7 Laue patterns from pure (011) specimen.

weld fusion zone of each specimen was observed by sectioning the cross section on a particular cross sectional plane in order to determine and compare the growth direction of the dendritic cell trunks with the crystallographic $\langle 100 \rangle$ direction.

Figures 8 (a) and (b) show the crystallographic orientations of three $\langle 100 \rangle$ axes in the fusion zone where the (001) and (011) specimens are cut along the plane (100), and the same directions for (111) surface specimen along the (011) plane are shown in Fig. 8 (c). In the case of the (001) specimen, two $[100]/[010]$ cross directions exist on the (001) surface and one $[001]$ direction is perpendicular to the (001) surface, and for (011) specimen, one $\langle 100 \rangle$ direction is on the surface and other two $[010]/[001]$ are 45° upward on the (100) plane. For the (111) specimen, the orientation $\langle 100 \rangle$ is 35.3° upward on the (011) plane.

Figures 9, 10 and 11 show schematic illustration of characteristic microstructure and $\langle 100 \rangle$ directions in the fusion zones, and the three photomicrographs of the laser weld zones in Al-2%Cu specimens with three specific



(a) (001) specimen.

(b) (011) specimen

(c) (111) specimen

Fig. 8 Schematic relationship between surface crystallographic orientation of specimens and $\langle 100 \rangle$ preferred growth direction of dendrites for (a) (001), (b) (011) and (c) (111) surfaces.

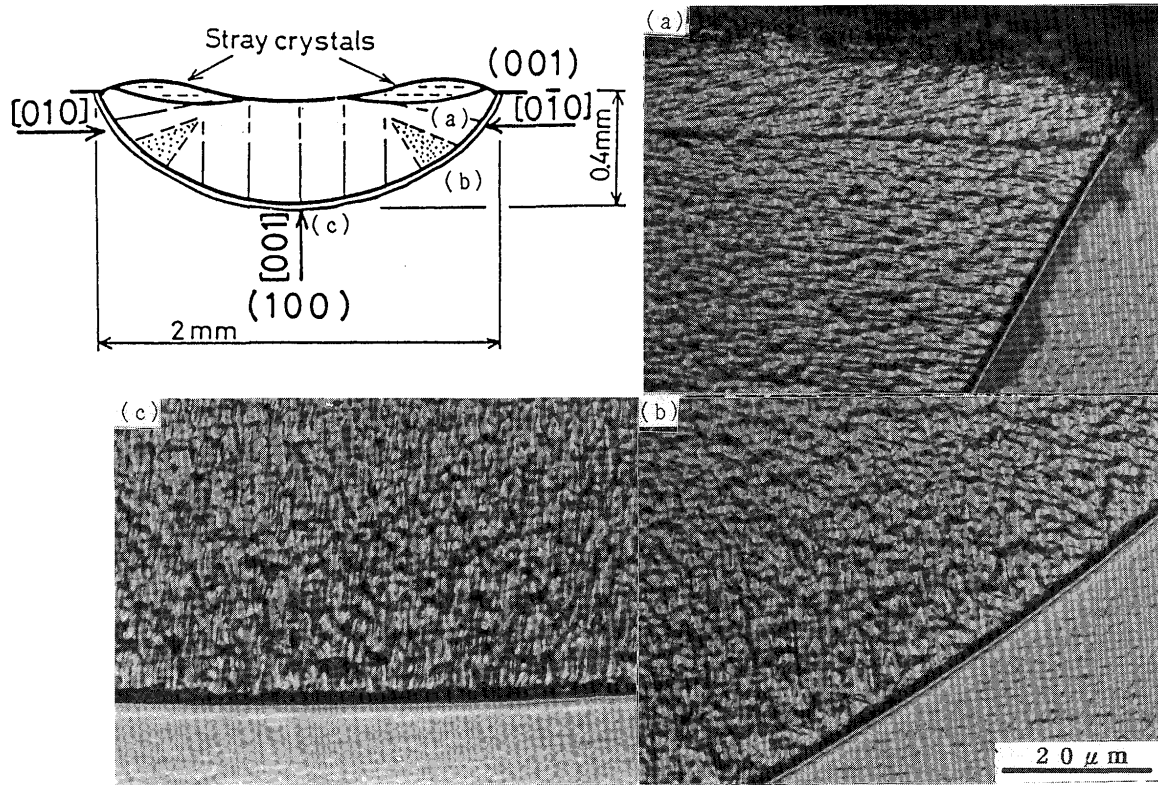


Fig. 9 (100) cross-sectional photomicrographs of Nd:YAG laser spot welded Al-2%Cu specimen of (001) surface. ($f_d = +5\text{ mm}$, $E_1 = 75\text{ J/P}$).

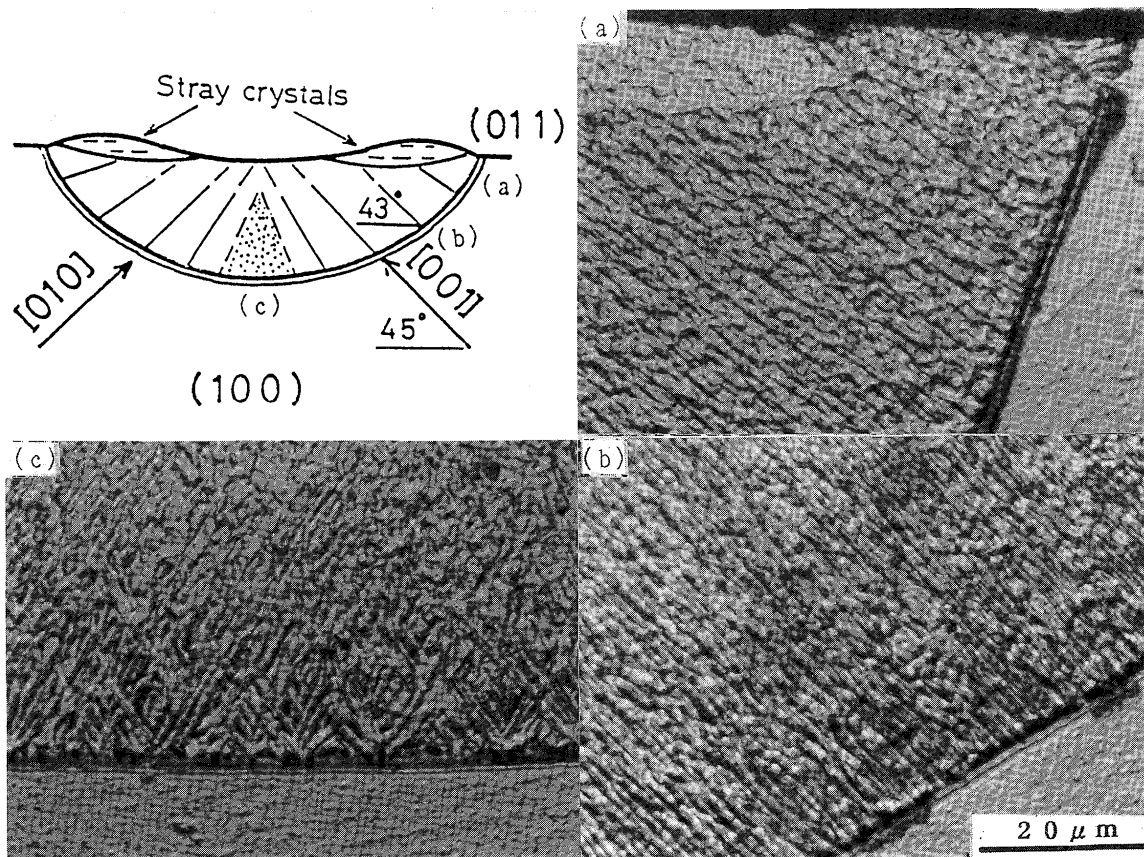


Fig. 10 (100) cross-sectional photomicrographs of Nd:YAG laser spot welded Al-2%Cu specimen of (011) surface.

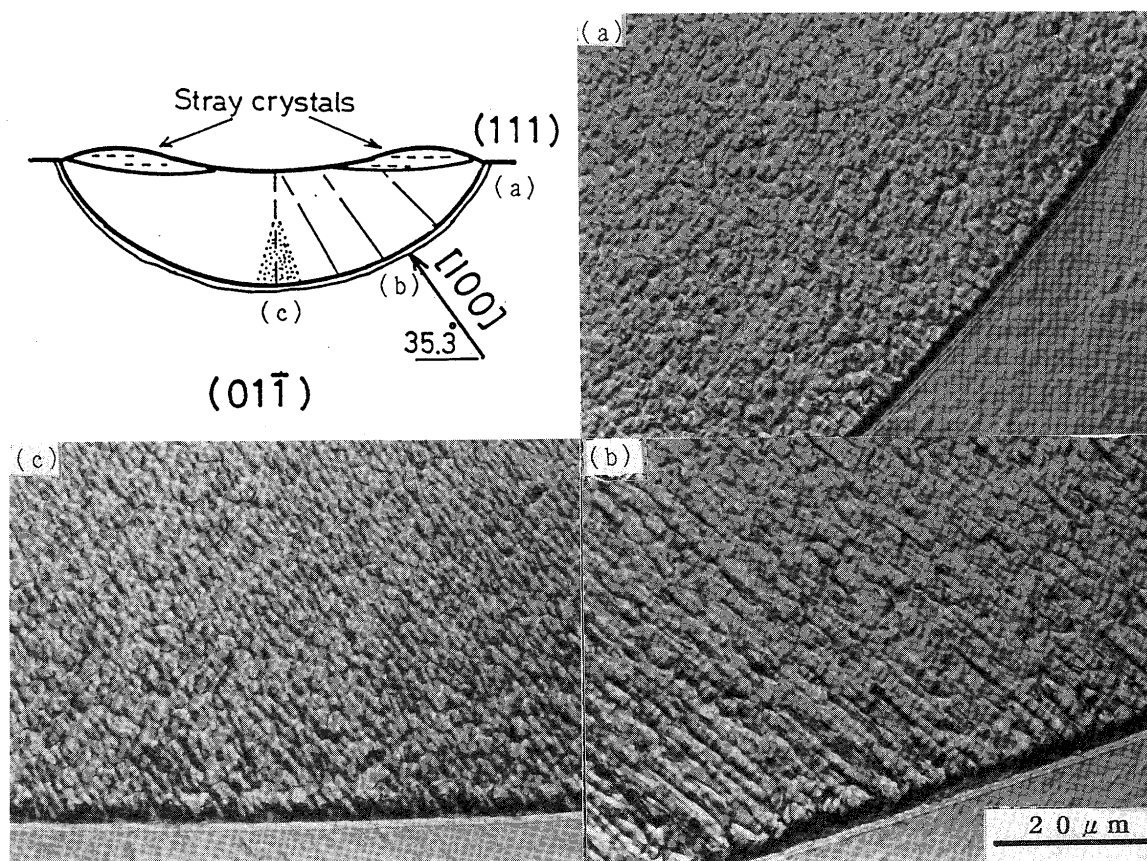


Fig. 11 (011) cross-sectional photomicrographs of Nd: YAG laser spot welded Al-2%Cu specimen of (111) surface.

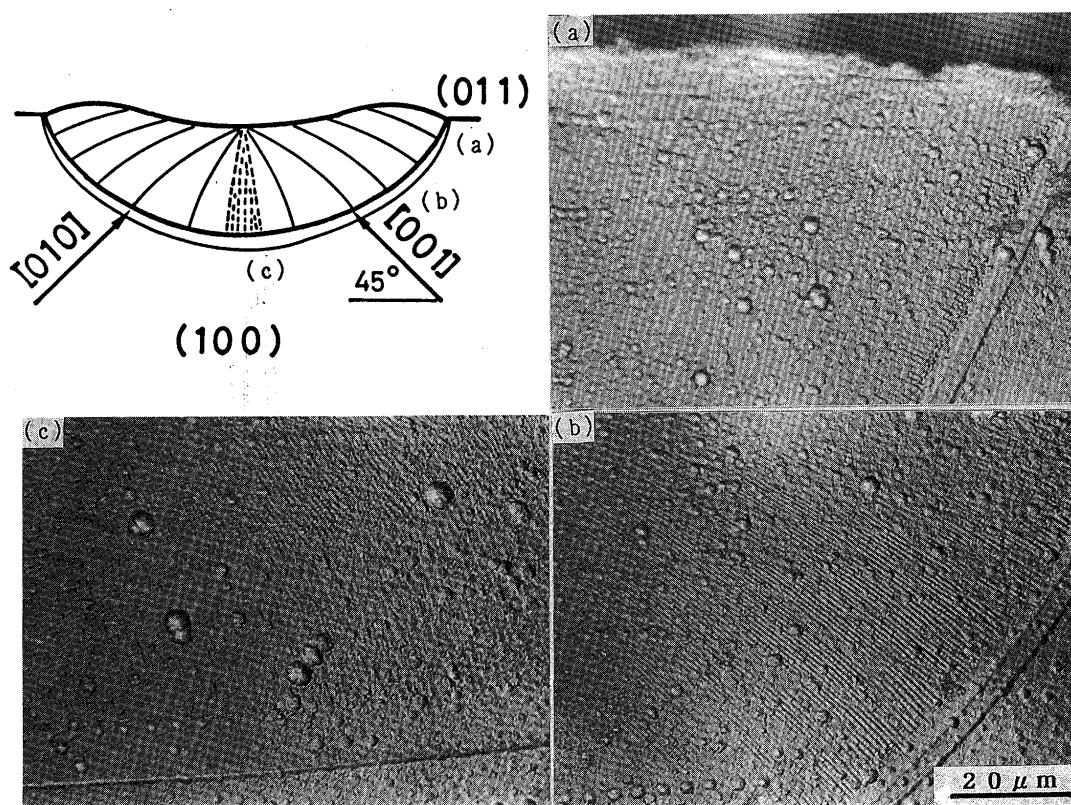


Fig. 12 (100) cross-sectional photomicrographs of Nd: YAG laser spot welded pure Al specimen of (011) surface.

(001), (011) and (111) plane surfaces, respectively (at $f_d = +5$ mm). Figure 12 shows a schematic representation of cross-sectional fusion zone and the photomicrographs of the laser weld zone in pure Al specimen with the (011) surface and (100) cross section under the same conditions. Planar interface solidification took place along the fusion boundary in every specimen. The distance of planar interface solidification appears to be longer in pure Al than in Al-2%Cu. Then cellular or cellular dendritic interface growth occurs inside the fusion zones. The cell sizes were in the range of 1 to 3 μm in Al-2%Cu specimens, and it suggests that the cooling rate estimated from the cell sizes is faster than 10^3 K/s or over^{34,35}.

The heat flow in the vicinity of the fusion zone can be assumed in the direction normal to the planar interface. Figure 13 shows the relationship between χ and ψ for Al-2%Cu (011) specimen at (100) cross section, where χ is the angle between the growth direction of cellular dendritic trunks and crystallographic $\langle 100 \rangle$ direction, and ψ is the angle between the perpendicular axis to the planar solidification interface and the $\langle 100 \rangle$ direction. If the heat flux has no influence upon the growth direction of cell trunks, all marks should be plotted on the transverse axis in Fig. 13, meaning that all cells or dendritic cells grow in exact preferred growth $\langle 100 \rangle$ direction. As shown in Fig. 13, when the angle between the direction of heat flux and the crystallographic $\langle 100 \rangle$ direction is small (ψ is small below about 10 deg), the cells or dendritic cells grow straight along the $\langle 100 \rangle$ direction. On the other hand, at higher ψ angle, χ increases with an increase in the ψ angle, thus causing a deviation of 15° at the maximum. That is, the heat flux affects the growth direction of dendritic cell trunks in the laser fusion zone of Al-2%Cu irrespective of rapid solidification.

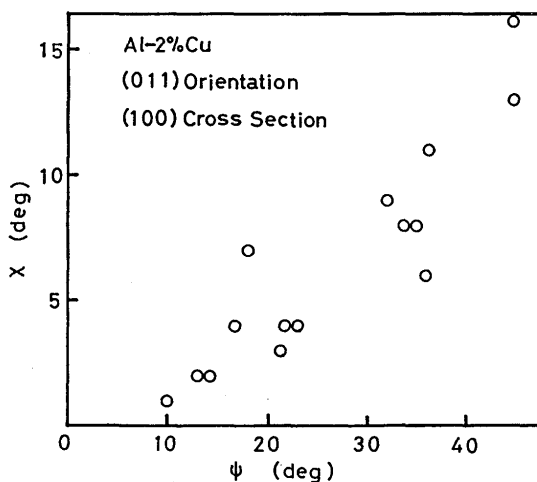


Fig. 13 Relationship between χ and ψ in Al-2%Cu alloy of (011) surface orientation and (100) cross section.

Matsuda, et al²³⁻²⁶ reported that the cellular dendrites varied its growth direction gradually toward the heat flux direction during solidification, on the basis of the observation of solidification structure in commercially available pure Al sheet produced by TIG arc welding. In the present work on laser spot welding of pure Al, the cellular dendrite did similarly change its growth direction gradually to the direction of heat flux during its growth. On the other hand, dendritic cells in Al-2%Cu changed its growth direction under the influence of heat flux immediately after planar solidification, and showed straight cellular (dendritic) growth afterwards. The straight growth of cell trunks and the deviation of growth direction to heat flux as great as 15° are characteristic of alloys such as Al-2%Cu and may be attributed to extremely slow growth velocity in the initial stages of solidification after planar growth as well as rapid solidification in the later growth stages.

In the boundary area where two $\langle 100 \rangle$ preferred growth directions impinge upon each other or have the same orientation to the heat flux, a peculiar structure zone containing net-like dendritic cells, so called "weave structure" was observed, and no clear grain boundaries caused by the intersection of different $\langle 100 \rangle$ directions were present.

Figures 14 (a) and (b) show SEM photos at higher magnification of the areas in Figs. 10 (a) and (c). There are fine granular and globular products (as white phases in the photo) along the cell boundaries. EDX analytical results of the center of a cell trunk and such a fine product are shown in Fig. 15. The granular product shows a higher peak of Cu and consequently includes higher Cu content than the central portion of the cell trunks. This suggests that the fine globular products in the cellular dendrite boundaries are of θ phase (Al_2Cu). This also indicates that the microsegregation of Cu cannot be prevented completely even by the laser rapid solidification (at the quenching rate of more than 10^3 K/s) in this experiment.

3.2 Microstructure of key hole type penetration welds

Figure 16 shows the (100) cross-sectional photomicrographs of the laser spot welded zones in (011) surface specimens of pure Al (a) and Al-2%Cu (b) single crystals (at higher power density at $f_d = 3$ mm). In both alloys, deep penetration of a spot weld (of about 1.2 mm depth) was obtained. A number of new grains are observed in the wide central part of the fusion zone in Al-2%Cu, but not in pure Al. These grains may be formed as "stray crystals". Large cracks were also present along grain boundaries in Al-2%Cu weld although no cracks were seen in pure Al weld. The Laue patterns from the surfaces of these laser spot welds are represented in Fig.

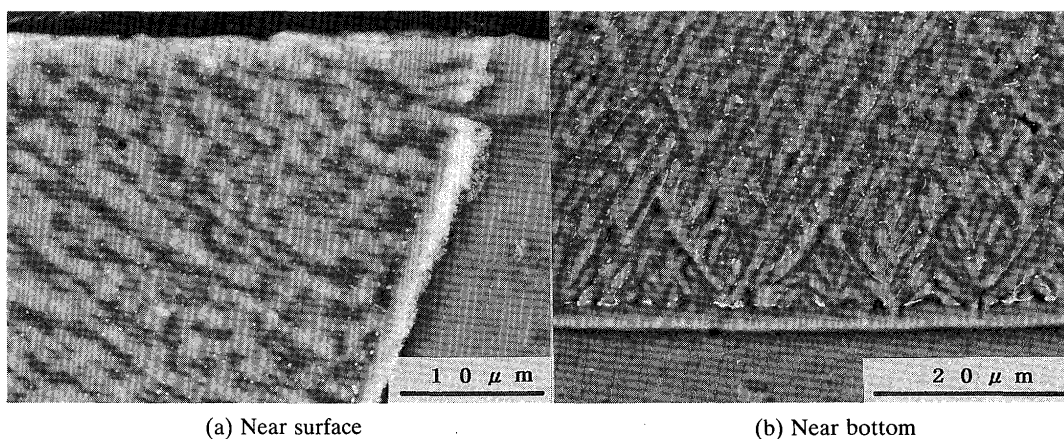


Fig. 14 (100) cross-sectional SEM micrographs of Nd: YAG laser spot welded Al-2%Cu specimen of (011) surface.

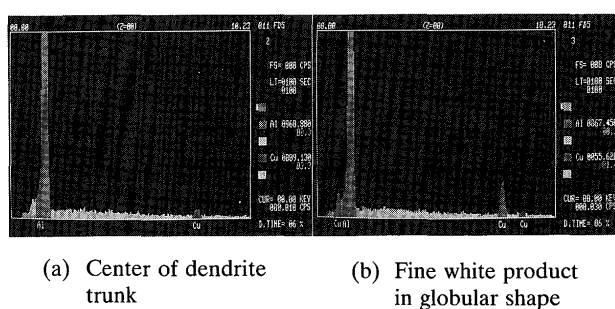
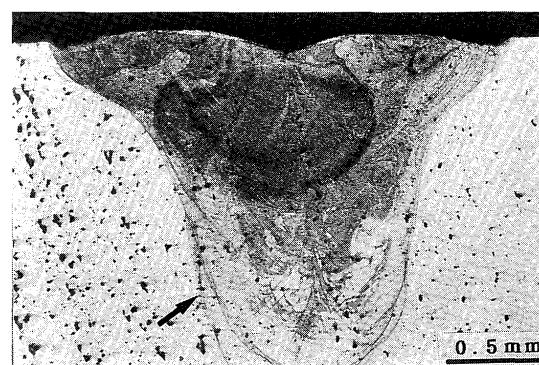
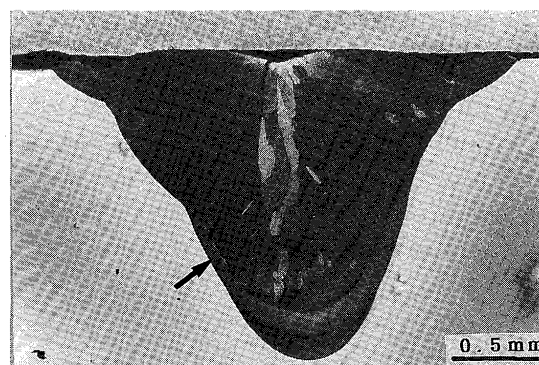


Fig. 15 EDX analysis results.



(a) Pure Al



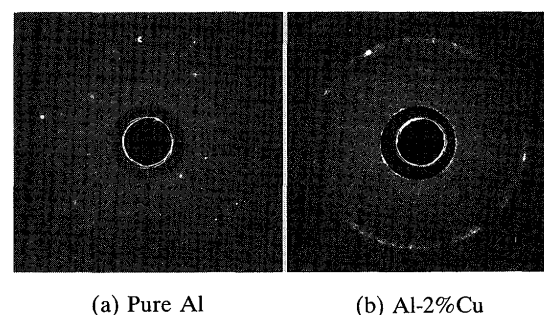
(b) Al-2%Cu

Fig. 16 (100) cross-sectional photographs of Nd: YAG laser spot welded (011) surface specimen ($f_d = +3$ mm, $E_1 = 75$ J/P).

17. For the laser deep penetration weld of pure Al, the reflection spots are seen and they are almost equal to those of the single crystal substrate. On the other hand, for Al-2%Cu, Debye-ring is observed, and there are several distinct, irregular reflection spots in the ring, suggesting that the sizes of grains are larger and the number is smaller in deep welds than in shallow welds. In addition, it is interesting to note that new grains appear to have the same orientation as the substrate and show monocrystallinity in a deep weld of Al-2%Cu on the whole.

Figure 18 shows higher magnification photomicrographs of the areas indicated by arrows in Fig. 16. An array of cells growing upward the right and the traces of multiple solidification (which may be due to intensive molten flow and sometimes correspond to ripple line in normal welding) are observed in both specimens. In Al-2%Cu, the molten flow might be so strong as to remelt the planar solidification region and to provide origins of "stray crystals", resulting in no continuity of cellular dendritic growth in re-solidified region.

Figures 19 (a), (b) and (c) show the surface appearances of the laser spot weld fusion zones of deep penetration in Al-2%Cu specimens of three different orientations. The crystallographic orientations of $\langle 100 \rangle$ are also indicated. Cracks were seen on the surface near the area between the $\langle 100 \rangle$ directions. It is interesting to



(a) Pure Al

(b) Al-2%Cu

Fig. 17 Laue patterns from spot welded surface.

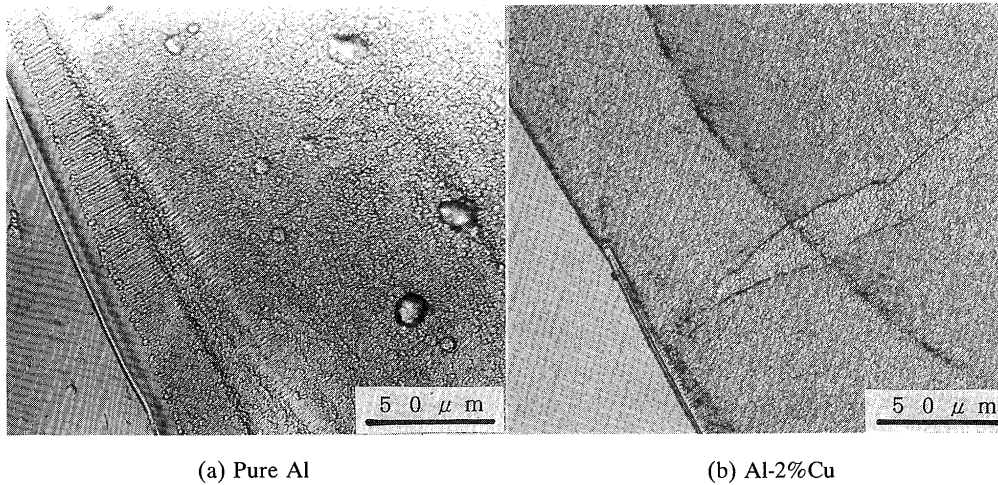


Fig. 18 Higher magnification photos of Figs. 16 (a) and (b), showing weld fusion zone microstructure near fusion boundary.

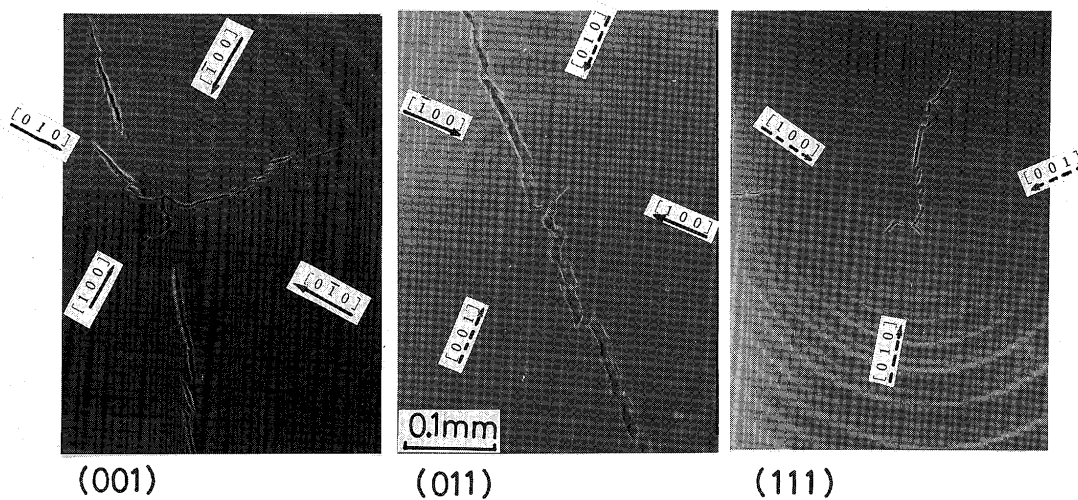


Fig. 19 Photographs of specimens with three orientations, showing cracks and $\langle 100 \rangle$ orientation.

understand that cracking occurred near the cell-impinging areas, probably because strains and stresses should be accumulated due to the solidification of $\langle 100 \rangle$ directions.

3.3 Role of grain boundary on cracking

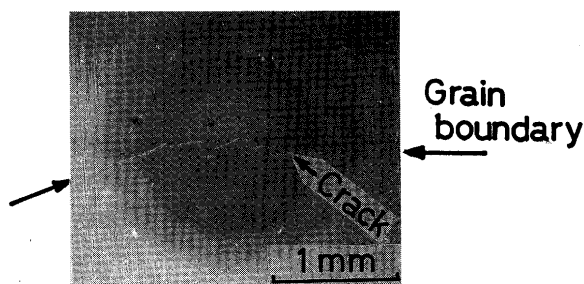
In order to confirm the cracking location in the microstructure, an additional experiment was performed by producing a laser spot weld of shallow penetration across the grain boundary in Al-2%Cu. **Figures 20** (a) and (b) show SEM photos of the surface appearance of a laser spot weld across the grain boundary and the fracture surface of cracks observed near the fusion boundary, respectively. Cracking occurred along the grain boundary, and its fracture surface morphology was dendritic, indicating that cracking was solidification cracking in the fusion zone and liquation cracking in the HAZ.

It was generally observed that the tendencies of

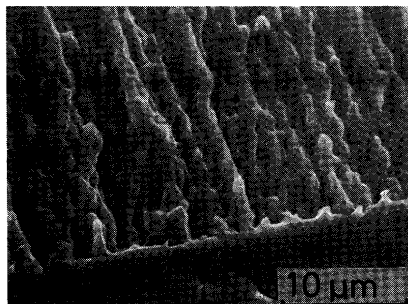
segregation and θ phase formation between the columnar grain boundaries and cellular dendritic boundaries was almost the same. However, the shape of low-melting liquid at boundaries may be affected by larger interface energy for the grain boundary³⁶⁾. Hemsworth, et al³⁷⁾. described that cracking occurred along cell boundaries as well as grain boundaries. However, it is solidification and liquation cracking along grain boundaries that constitute cracking in a laser spot weld of Al alloy subjected to rapid solidification.

4. Conclusions

In order to obtain a basic knowledge of rapid solidification of alloys, a pulsed Nd: YAG laser was irradiated onto the single crystals of pure Al and Al-2%Cu alloys. Thus investigation was made concerning the



(a) Specimen surface



(b) Crack surface

Fig. 20 Typical hot cracking along grain boundary when laser spot weld was produced on boundary of two crystals.

mechanism of rapid solidification, microsegregation, the characteristics of microstructure and the crystallographic orientation dependency of cell trunks and solidification cracking paths in the rapidly solidified zone. The results obtained in this study are summarized as follows:

- (1) In the case of pure Al, laser spot weld fusion zones had the same crystallographic orientation as the substrate and retained the monocrystallinity independently of the penetration depth.
- (2) In the case of Al-2%Cu, most of the laser spot fusion zone solidified nearly in the preferred growth $\langle 100 \rangle$ orientation as straight trunks of dendritic cells. In an area where the $\langle 100 \rangle$ direction deviated largely from the direction of heat flux, dendritic cell trunks generating just after the planer interface growth were deviated, and the maximum deviation measured was 15° from the $\langle 100 \rangle$ toward the direction of heat flux.
- (3) A number of stray crystals were observed in Al-2%Cu specimen but not in pure Al. In the heat conduction type fusion zone of shallow penetration, stray crystals were present near the surface area. In the key hole type fusion area of deep penetration, stray crystals were mainly observed at the central portion. This was attributed to intensive molten flow in an alloy with some contents of solute elements.
- (4) The net-like or weave structure of cellular dendrites was observed in the heat conduction type solidifica-

tion boundary area where many cells with several $\langle 100 \rangle$ directions intersected each other and existed mixedly.

- (5) The maximum limit of solid solution of Cu in Al-Cu system is approximately 5.7% at 548°C , but it was observed that Cu segregated in cell and grain boundaries, resulting in the formation of θ phase even in the rapidly solidified portion of Al-2%Cu alloy. This is due to small distribution coefficient of Cu.
- (6) It was clearly confirmed that hot cracking of solidification cracking and liquation cracking occurred along grain boundaries but not at cell boundaries in Al-2%Cu alloy.

References

- 1) B. H. Kear, E. M. Breinan and L. E. Greenwald: "Laser Glazing-A New Process for Production and Control of Rapidly Chilled Metallurgical Microstructures", Metal Technology, Vol.6 (1979), 121-129.
- 2) "Rapid Solidification Processing: Principles and Technologies II," eds. R. Mehrabian, B. H. Kear and M. Cohen, Claitor's Publishing Division, Baton Rounge, LA, (1980) (Proc. 2nd Int. Conf. at Boston, VA, March 1980).
- 3) "Rapidly Solidified Amorphous and Crystalline Alloys," eds. B. H. Kear and B. C. Giessen, Elsevier North Holland, New York, (1982) (Proc. Mats. Res. Soc. Meeting at Boston, MA, Nov., 1981, Symposium F).
- 4) "Rapidly Quenched Metals IV," Eds. T. Masumoto and K. Suzuki, The Japan Institute of Metals, (1982) (Proc. 4th Int. Conf. at Sendai, Japan, Aug., 1981).
- 5) "Rapid Solidification of Metals and Alloys," H. Jones, Monograph #8, The Institution of Metallurgists, London, 1982.
- 6) "Laser Materials Processing," Ed. M. Bass, North Holland Publishing Company, (1983).
- 7) "Laser Surface Treatment of Metals", eds. C. W. Draper and P. Mazzoldi, Martinus Nijhoff Publishers, (1986) (Proc. of the NATO Advanced Study Institute on Laser Surface Treatment of Metals, San Miniato, Italy, Sept., 2-13, 1985).
- 8) B. H. Kear and P. R. Strutt: "Rapid Solidification Surface Modification of Materials," Ed. R. Bakish, Bakish Materials Corporation, (1984), 234-251.
- 9) H. A. Davies: "Rapid Quenching Techniques and Formation of Metallic Glasses", in "Rapidly Quenched Metals III", Ed. B. Cantor, The Metal Society, London, Vol.1 (1978), 1-21.
- 10) G. W. Roper: "Exploitation of Metallic Glasses Through Surface Engineering", Surface Engineering, Vol.1 (1985), No.4, 289-296.
- 11) S. Katayama and A. Matsunawa: "Solidification Microstructure of Laser Welded Stainless Steels", Proc. ICALEO '84, L. I. A., Boston, MA, USA, Nov., Vol.44 (1984), 60-67.
- 12) S. Katayama and A. Matsunawa: "Solidification Behavior and Microstructural Characteristics of Pulsed and Continuous Laser Welded Stainless Steels", ed. C. Albright, Proc. ICALEO '85, IFS and Springer-Verlag, Berlin, San Francisco, Nov., (1985), 19-25.
- 13) A. Matsunawa, S. Katayama, Y. Ohmi and T. Kuroki: "Formation of Amorphous Alloy Layer by Pulsed Laser", Proc. LAMP '87, High Temperature Society of Japan, Osaka, Japan, May (1987), 441-446.
- 14) A. Matsunawa, S. Katayama, Y. Ohmi and T. Kuroki: "Pulsed Laser Glazing of Alloy Surface", Proc. CISFEL,

- Cannes, Sept., (1988), 563-572.
- 15) R. Mehrabian: "Rapid Solidification", *International Metals Reviews*, Vol.27 (1982), No.4, 185-208.
 - 16) W. Kurz, B. Giovanola and R. Trivedi: "Theory of Microstructural Development during Rapid Solidification", *Acta Metall.*, Vol.34 (1986), 823-830.
 - 17) R. Trivedi and W. Kurz: *Acta Metall.*, Vol.34 (1986), 1663-1670.
 - 18) W. Kurz and D. J. Fisher: "Fundamentals of Solidification", Trans Tech Publications, Ltd., Switzerland, (1984).
 - 19) W. A. Tiller and J. W. Rutter: "The Effect of Growth Conditions upon Solidification of a Binary Alloy", *Can. Journal of Physics*, Vol.34 (1956), 96-100.
 - 20) E. Teghtsoonian and B. Chalmers: "The Macroscopic Structure of Tin Single Crystals", *Can. J. Phys.*, Vol.29 (1951), 370-381.
 - 21) E. Teghtsoonian and B. Chalmers: "Further observations on the Macromosaic Structure of Tin Single Crystals", *Can. J. Phys.*, Vol.30 (1952), 388-401.
 - 22) H. A. Atwater and B. Chalmers: "The Influence of Impurities on the Macromosaic Structures of Tin and Lead", *Can. J. Phys.*, Vol.35 (1957), 208-251.
 - 23) F. Matsuda and T. Hashimoto and T. Senda: "Fundamental Investigation on Solidification Structures in Weld Metal", *Trans. NRIM*, Vol.11, (1969), No.1, 43-58.
 - 24) H. Nakagawa, M. Katoh, F. Matsuda and T. Senda: "X-ray Investigation on Solidification Structures in Weld Metal", *Trans. JWS*, Vol.1 (1970), No.1, 94-103.
 - 25) H. Nakagawa, M. Katoh, F. Matsuda and T. Senda: "Fundamental Solidification Mechanism and Microstructures in GTA Spot Welds of Aluminum Sheets", *Trans. JWS*, Vol.1 (1970), No.2, 28-39.
 - 26) H. Nakagawa, M. Katoh, F. Matsuda and T. Senda: "Crystallographic Investigation for Origination of New Columnar Crystal in Aluminum Weld Metal Using Single Crystal Sheet", *Trans. JWS*, Vol.2 (1971), No.1, 1-9.
 - 27) W. F. Savage, C. D. Lundin and A. H. Aronson: "Weld Metal Solidification Mechanics", *Welding Journal*, Vol.44 (1965), 175s-181s.
 - 28) W. F. Savage, and A. H. Aronson: "Preferred Orientation in the Weld Fusion Zone", *Welding Journal*, Vol.45 (1966), 85s-89s.
 - 29) W. F. Savage: "Solidification, Segregation and Weld Imperfection", *Welding in the World*, Vol.18(5/6) (1980), 89-104. 175s-181s.
 - 30) S. Kou and Y. Lee: "Grain Structure and Solidification Cracking in Oscillated Arc Welds of 5052 Aluminum Alloy", *Metall. Trans.*, Vol.16A (1985), 1345-1352.
 - 31) S. A. David and J. M. Vitek: "Correlation between Solidification Parameters and Weld Microstructures", *International Materials Reviews*, Vol.34 (1989), No.5, 213-245.
 - 32) S. L. Narasimhan, S. M. Copley, E. W. Van Stryland and M. Bass: "Solidification of a Laser Melted Nickel-Base Superalloy", *Metall. Trans. A*, Vol.10A, (1979), 654-655.
 - 33) M. Rappaz, S. A. David, J. M. Vitek and L. A. Boatner: *Metall. Trans. A*, Vol.20A, (1989), 1125-1138.
 - 34) H. A. Pallacio, M. Solari and H. Biloni: "Microsegregation in Cellular dendritic Growth in Binary Alloys of Al-Cu", *J. of Crystal Growth*, Vol.73 (1985), 369-378.
 - 35) K. P. Yound and D. H. Kirkwood: "The Dendrite Arm Spacings of Aluminum-Copper Alloys Solidified Under Steady-State Conditions", *Meta. Trans. A*, Vol.6A (1975), 197-205.
 - 36) H. Nakagawa, F. Matsuda and T. Senda: "Effect of Sulphur on Solidification Cracking in Weld Metal of Steel (Report I)", *Trans. JWS*, Vol.5 (1974), No.1, 39-46.
 - 37) B. Hemsworth, T. Boniszewski and N. F. Eaton: "Classification and Definition of High Temperature Welding Cracks in Alloys", *Metal Construction and British Welding Journal*, Vol.1 (1969), No.2, 5-16.